

Article

Effects of Plot Size on Airborne LiDAR-Derived Metrics and Predicted Model Performances of Subtropical Planted Forest Attributes

Chungan Li ^{1,*} , Xin Lin ^{1,2}, Huabing Dai ², Zhen Li ² and Mei Zhou ³¹ Forestry College, Guangxi University, 100, East Daxue Rd., Nanning 530004, China² Guangxi Forest Inventory & Planning Institute, 14, Zhonghua Rd., Nanning 530011, China³ School of Computer, Electronic and Information, Guangxi University, 100, East Daxue Rd., Nanning 530004, China

* Correspondence: chungan@gxu.edu.cn

Abstract: Investigating the impact of field plot size on the performance of estimation models for forest inventory attributes could help optimize the technical schemes for an operational airborne LiDAR-assisted forest resource inventory. However, few studies on the topic have focused on subtropical forests. In this study, 104 rectangular plots of 900 m² (subdivided into nine quadrats with an area of 10 × 10 m) in subtropical planted forests (Chinese fir, pine, eucalyptus, and broad-leaved forest, 2–56 years old) were used to establish four datasets with six different plot sizes (100, 200, 300, 400, 600, and 900 m²) by combining quadrats. The differences in the LiDAR-derived metrics and forest attributes between plots of different sizes were statistically analyzed. Based on the multivariate power models with stable structures, the differences in estimation accuracies of the stand volume (VOL) and basal area (BA) using plot data of different sizes were compared. The results indicated that: (1) the mean differences in LiDAR-derived metrics of the plots of different sizes in all forest types were small, and most of them had no statistically significant differences ($\alpha = 0.05$) between the plots of different sizes and the 900 m² plots; however, the standard deviation of the difference increased rapidly with decreasing plot size; (2) except for the maximal tree height of the plots, the other forest attributes, including the mean tree height, diameter at breast height, BA, and VOL of all forest types, showed no statistically significant differences between the plots of different sizes and the 900 m² plots; and (3) with increasing plot size, the accuracies of VOL and BA estimations improved markedly, and the effects of plot size on the estimation accuracies of the different forest attributes and different forest types were essentially the same. Spatial averaging resulted in the variations in the independent variables (LiDAR variables) and dependent variables (forest attributes) decreasing gradually with the increasing plot size, which was the main reason for the model's accuracy improving. In applying airborne LiDAR to a large-scale subtropical planted forest inventory, the plot size should be at least 600 m² for all forest types.

Keywords: forest inventory; airborne LiDAR; rectangular plot; accuracy; spatial averaging

Citation: Li, C.; Lin, X.; Dai, H.; Li, Z.; Zhou, M. Effects of Plot Size on Airborne LiDAR-Derived Metrics and Predicted Model Performances of Subtropical Planted Forest Attributes. *Forests* **2022**, *13*, 2124. <https://doi.org/10.3390/f13122124>

Academic Editors: Chinsu Lin and Wenzhi Liao

Received: 28 October 2022

Accepted: 8 December 2022

Published: 11 December 2022

Publisher's Note: MDPI stays neutral with regard to jurisdictional claims in published maps and institutional affiliations.



Copyright: © 2022 by the authors. Licensee MDPI, Basel, Switzerland. This article is an open access article distributed under the terms and conditions of the Creative Commons Attribution (CC BY) license (<https://creativecommons.org/licenses/by/4.0/>).

1. Introduction

Airborne laser scanning (ALS; also referred to as Light Detection and Ranging (LiDAR)) can measure distances accurately, penetrate the forest canopy [1], and provide accurate information characterizing the three-dimensional (3D) structure of a forest canopy [2]. Based on the statistical relationships between airborne LiDAR- or UAV-derived metrics (e.g., the height and density percentiles of the laser point clouds) and forest attributes (e.g., mean diameter at breast, DBH; mean stand height, H; basal area, BA; stand volume, VOL; and aboveground biomass, AGB) measured in field plots, we could accurately estimate forest inventory attributes and efficiently generate wall-to-wall maps [3]. Therefore, airborne LiDAR has been widely applied in large-scale operational forest inventories since 2002 [4,5].

Thus, it is a transformative technology for forest inventory and ecological monitoring [6]. The area-based approach (ABA) is widely used for airborne LiDAR-based forest attribute estimation. However, the effects of growth competition on attribute estimation have been addressed in recent years [7,8]. Meanwhile, UAVs (with LiDAR and optics) have also been used for small-scale forest research [9,10].

The cost of airborne LiDAR-based forest inventory is determined mainly by point density, sample size, and plot size. In particular, the point density, which depends on the flight height, speed, and width of the laser-scanning line strip, determines the cost of LiDAR data acquisition; the sample size (number of plots) and plot size affect the field measurement cost. Therefore, while ensuring an acceptable estimation accuracy of forest inventory attributes, optimizing these technical parameters is essential to reducing inventory costs. Numerous studies have examined how the point density affects the accuracy of the airborne LiDAR estimation of forest attributes based on the area-based approach [11–13]. Watt et al. suggested that if the number of point clouds in a field plot exceeded 100, the R^2 did not change significantly [1]. In a large-scale operational forest inventory in Norway, the point density was approximately $0.7 \text{ points m}^{-2}$ [14]. Because of the limited amount of available field data, very few studies have addressed how sample size affects the accuracy of estimating forest attributes with airborne LiDAR [15]. By performing Monte Carlo simulations, Gobakken and Næsset found that when the sample size decreased by 75% and even 50% from the original numbers of 50, 34, and 48, the estimation accuracy of forest attributes was moderately reduced [11]. When LiDAR data were used as prior information for stratified sampling, the minimum sample size was approximately 50 for each stratum in Norway [14]. However, only a few studies have focused on how the plot size affects the estimation accuracy of forest attributes. Gobakken and Næsset discovered that as the plot size increased from 200 m^2 to $300\text{--}400 \text{ m}^2$, the model accuracy improved when a regression model was applied to estimate the mean stand height, basal area, and stand volume [11]. A study indicated that when the point density exceeded $0.5 \text{ points m}^{-2}$ and the plot size exceeded 400 m^2 , the R^2 of the stand volume model was very stable [1]. In the productive forests in Norway, as the plot size increased from $200\text{--}250 \text{ m}^2$ to $1000\text{--}4000 \text{ m}^2$, the RMSE or standard deviation decreased from 20%–25% to 10%–15% [4,16,17]. Zolkos et al. analyzed over 70 published papers on estimating aboveground biomass using different remote sensing platforms (airborne and satellite-borne) and sensor types (optical, radar, full waveform LiDAR, and discrete return LiDAR). They found a robust and clear correlation between model error and plot size. As the plot size increased, the model error rapidly decreased [18]. Although the community already knows about the effect of plot size, previous studies have focused mainly on temperate forests and circular plots. Moreover, the mechanism of the effect of plot size on the model accuracy of forest attribute estimation has not been fully revealed. Therefore, further in-depth studies are needed for different forest types (tropical and subtropical forest, planted forest, etc.), different forest parameters (basal area, stand volume, etc.), and different plot shapes (round or square). More importantly, the mechanism of the effect of plot size on the prediction accuracy of forest attributes needs to be investigated.

To provide additional evidence for optimizing the technical schemes of the airborne LiDAR-based forest inventory, the present study focuses on subtropical planted forests. The specific objectives are: (1) to investigate the effects of plot size on LiDAR-derived metrics and measure forest attributes of different forest types; (2) to analyze the plot size effects on the model performance in estimating the BA and VOL of various forest types; (3) to investigate the mechanism of plot size effects on the model accuracy of attribute estimation for different forest types; and (4) to determine a suitable plot size for the large-scale airborne LiDAR-assisted subtropical planted forest resource inventory.

2. Materials and Methods

2.1. Study Area

The study site was located at the state-owned Gaofeng Forest Farm in the southern part of Guangxi Zhuang Autonomous Region of southern China. Shaped as a rectangle from northeast to southwest, the length and width of the study site were 11.2 km and 4.2 km, respectively, and the area covered approximately 4770 ha (Figure 1).

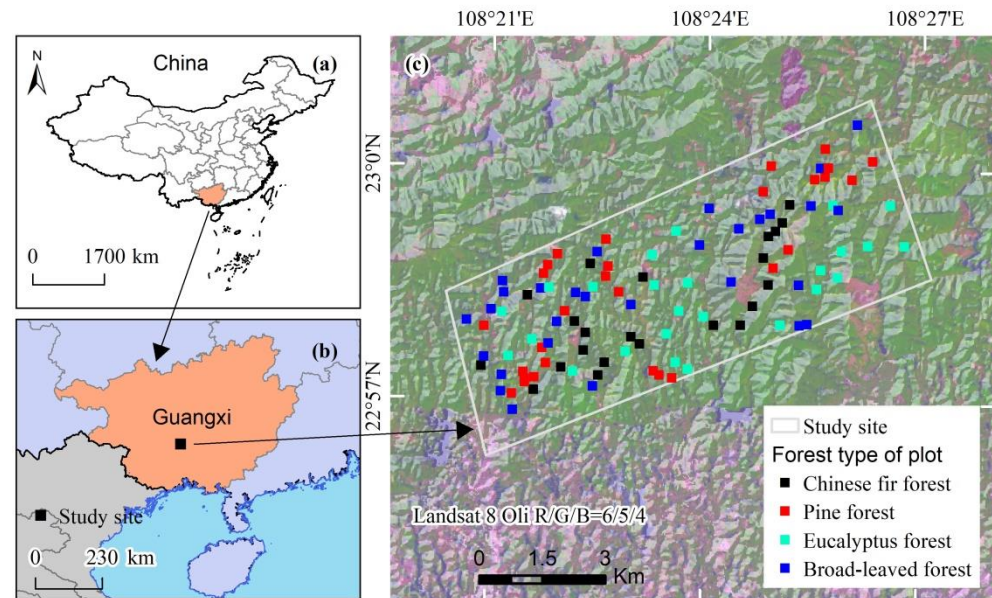


Figure 1. (a) Location of the Guangxi Zhuang Autonomous Region in China; (b) Location of the study site in Guangxi; (c) Distribution of the field plots.

The study area is characterized by hilly terrain. With elevations of 90–460 m, the study area had slopes of 15–65°, with approximately 70% of the areas between 25° and 35°. Lying south of the Tropic of Cancer, the region has a humid subtropical monsoon climate, with an average annual temperature of 21.6 °C, an average annual rainfall of 1300 mm, and an average annual relative humidity of 79%. Approximately 95% of the forests in the region are planted forests. Most forest stands were planted over 15 years ago, except for the eucalyptus plantations, which are 2–9 years old. The main tree species in the area include *Eucalyptus urophylla*, *E. grandis* × *E. urophylla*, *Pinus massoniana*, *P. elliottii*, *Cunninghamia lanceolata*, *Illicium verum*, *Castanopsis hystrix*, *Michelia macclurei*, *M. odora*, *Magnolia sumatrana*, *Tilia tuan*, *Mytilaria laosensis*, and *Acacia crassicarpa*. Among them, the industrial eucalyptus plantations and anise forests are pure forests. The remaining 60% of the forest stands are artificial or natural mixed forests.

2.2. Field Plot Data

Field plots were measured from October 2016 to February 2017. According to the dominant species, the forests were categorized into four types (strata), i.e., the Chinese fir, pine, eucalyptus, and broad-leaved forests. Each forest type had 22–29 field plots, totaling 104 plots.

The setting and measurement of the field plot are described below: (1) the field plot size was 30 × 30 m (900 m²), all setting in a north-south orientation, and was subdivided into nine quadrats of 10 × 10 m; (2) a compass and a laser rangefinder (Leica DISTO™ X30) were employed to set and measure the plot and quadrats, and their boundaries were marked with nylon ropes; (3) within each quadrat, DBH (1.3 m) of all live trees greater than 5 cm, as well as the tree species, were measured and recorded. The heights of three average trees and the highest tree were measured using a Haglöf Vertex IV hypsometer; (4) the Trimble Global Navigation Satellite System (GNSS) receiver using a real-time kinematic

(RTK) positioning method was employed to position the northwestern and southeastern corners of the plot. Two RTK-GNSS instruments were used as base stations, which were located in a nearby open area. Using the post-correction approach, the positioning accuracy was better than 1 m. The coordinates of the corners of each quadrat were calculated by interpolation. The stand attributes of each quadrant included DBH, H, maximal height (Hm), BA, tree stem density (N), and VOL, which was calculated using BA and H with the local provincial species-specific allometric equations [19]. The forest stand attributes of field plots were determined based on those of the nine quadrants. The summary statistics of 900 m² plots are shown in Table 1.

Table 1. Summary of field measurements of the 900 m² field plots. CV is the coefficient of variation.

Stratum	Sample Size	Stand Age (yr)	DBH		Height		Max. Height (m)	BA		Tree Density (Stem ha ⁻¹)	VOL	
			Mean (cm)	CV (%)	Mean (m)	CV (%)		Mean (m ² ha ⁻¹)	CV (%)		Mean (m ³ ha ⁻¹)	CV (%)
Chinese Fir	22	19–28	15.04	14.78	13.37	13.41	16.45	24.78	19.75	1536	179.87	24.39
Pine	29	7–24	17.83	21.57	13.14	26.94	14.91	26.51	28.69	1166	175.86	42.34
Eucalyptus	25	2–9	11.11	15.26	16.02	20.99	18.67	17.6	35.42	1826	146.25	49.3
Broad-leaved	28	7–56	14.35	27.36	11.37	31.84	13.7	20.44	39.28	1343	128.74	59.24

To analyze the effects of plot size on the LiDAR metrics, measure forest attributes, and the accuracy of forest attribute estimation, the quadrats were combined into six plots of different sizes (100, 200, 300, 400, 600, and 900 m²). Four protocols for combination were used. A protocol is shown in Figure 2, and the other protocols are listed in Table 2.

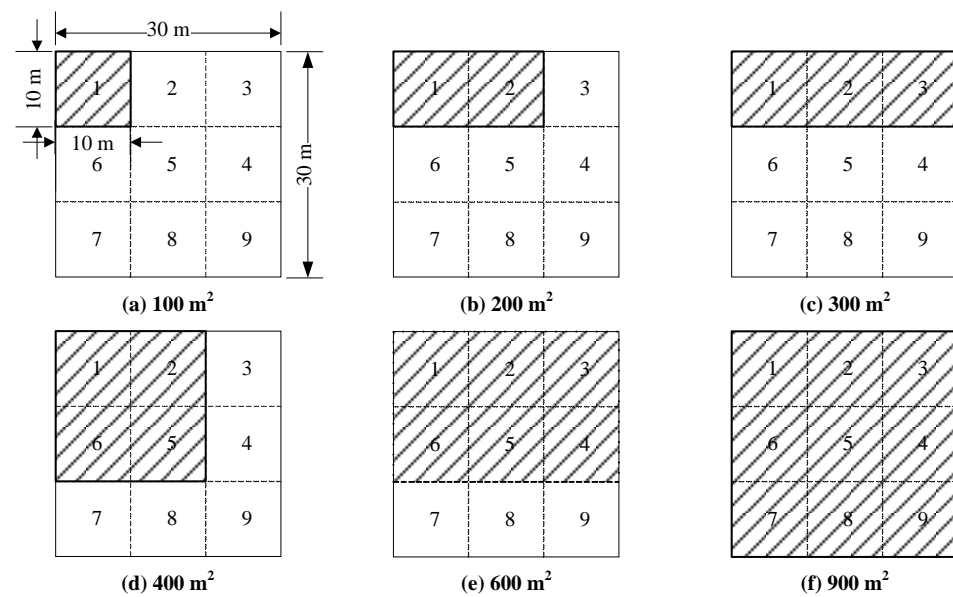


Figure 2. Layout of the sampling plot of 900 m² and protocol 1 for combining quadrats into plots of different sizes.

Table 2. Four protocols for combining quadrats into plots of different sizes.

Protocol	100 m ²	200 m ²	300 m ²	400 m ²	600 m ²	900 m ²
1	P1	P1, P2	P1, P2, P3	P1, P2, P5, P6	P1–P6	P1–P9
2	P2	P2, P5	P2, P5, P8	P2–P5	P2–P5, P8, P9	P1–P9
3	P6	P6, P7	P1, P6, P7	P5–P8	P1, P2, P5–P8	P1–P9
4	P5	P4, P5	P4–P6	P4, P5, P8, P9	P4–P9	P1–P9

Note: P1–P9 are quadrats 1–9.

As there were four combination protocols, we obtained four datasets containing plots of different sizes, in which each forest type had 22–29 field plots of different sizes. The following method was applied to calculate the forest attributes of each field plot based on the quadrats: for a plot with a given area (e.g., 400 m²), the BA and VOL were the sums of the corresponding values of the quadrats enclosed. For example, in protocol 1, the 400 m² plot enclosed quadrats 1, 2, 5, and 6 (Figure 1 and Table 2); in protocol 2, the 400 m² plot enclosed quadrats 2–5 (Table 2). The DBH and H were weighted averages of the BAs of the corresponding values of the quadrats enclosed, and Hm was the maximal height in all quadrats enclosed.

2.3. Lidar Data

Helicopter-borne LiDAR data were acquired in September 2016 using a Riegl VQ-1560 LiDAR scanner (Riegl Laser Measurement System, GmbH, Horn, Austria) at an altitude of 500 m and a speed of 90 km·h⁻¹, and the swath width was 350 m. The characteristics of the LiDAR sensor were as follows: the laser wavelength was near-infrared; the laser beam divergence was 0.5 mrad; the pulse emission frequency was 700 kHz; the scanning frequency was 820 kHz; the maximum scanning angle was ±30°. The final average point density was 3.2 points m⁻². The point clouds were geo-referenced to a projection system of the China Geodetic Coordinate System 2000 (CGCS2000). The mean square error of the laser point cloud height was less than 0.15 m. In the LiDAR data preprocessing, the TerraScan software (TerraSolid, Ltd., Helsinki, Finland) was used to label the point clouds as the ground return and non-ground return data using the adaptive triangulation network (TIN) filter algorithm. A digital terrain model (DTM) with a grid cell size of 2 m was finally generated using ground returns. Using this DTM, we removed the influence of topography and obtained DTM-normalized LiDAR point clouds.

According to the coordinates of the four corners of the 900 m² plot, we extracted the normalized point cloud data to calculate the LiDAR-derived metrics using the Python software package (Python version 2.8). The LiDAR-derived metrics included the height and density metrics, the mean leaf area density (LADmean) of the stand canopy, and its coefficient of variation (LADcv) [2]. Some researchers used the first LiDAR echoes to extract the metrics [13,20–22]. However, similar to most researchers [6,23–26], all echoes were used to extract thirteen LiDAR-derived metrics in this study. Based on the coordinates of the four corners of all quadrats, LiDAR point clouds were extracted in plots of different sizes, and the LiDAR-derived metrics were calculated using the same method as that used in the 900 m² field plot.

2.4. Comparative Analysis of Plot Size Effects

To evaluate the effects of plot size on LiDAR-derived metrics, the two-tailed paired *t*-test was employed to analyze the differences of the means of LiDAR-derived metrics between small plots (100, 200, 300, 400, and 600 m²) and 900 m² plots for all datasets and all forest types. These metrics included: mean point cloud height (Hmean); 25th, 50th, and 75th height percentiles (hp25, hp50, and hp75); maximum height (Hmax); CV of point cloud height distribution (Hcv); canopy cover (CC); 25th, 50th, and 75th density percentiles (dp25, dp50, and dp75); and LADmean and LADcv. Then, the number of statistically significant differences for each metric in the four datasets was statistically analyzed.

By employing a method similar to that described above, we analyzed the differences of the means of forest attributes (DBH, H, Hm, BA, and VOL) between plots of different sizes and the 900 m² plots for all four datasets and all forest types.

Forest attributes are closely related to the three-dimensional (3D) structures of their canopies [27]. To assess the impact of plot size on the model performance of stand attribute estimations, we constructed VOL and BA estimation models for all forest types using LiDAR-derived metrics that depict the 3D structure of the forest canopy. The model formulation is shown as follows [28]:

$$\hat{y} = a_0 Hmean^{a_1} CC^{a_2} LADcv^{a_3} Hcv^{a_4} dp50^{a_5} + \varepsilon \quad (1)$$

where \hat{y} is the estimated VOL or BA, a_0, a_1, \dots , and a_5 are the model parameters, and ε is the estimation error. To evaluate the reliability of the models, leave-one-out cross-validation (LOOCV) was applied because only a few field plots were available, which could not provide an independent validation dataset for all forest types. The three pointwise goodness-of-fit statistics, R^2 , rRMSE, and mean predictive error (MPE), were computed and applied to assess the models. The formula for the MPE is shown below [29,30]:

$$MPE = t_\alpha \times (SEE/\bar{y})/\sqrt{n} \times 100 \quad (2)$$

where $SEE = \sqrt{\sum (y_i - \hat{y}_i)^2 / (n - p)}$ is the standard deviation of the estimate, y_i is the observed value, \hat{y}_i is the estimate, \bar{y} is the mean of y_i , n is the number of field plots, p is the number of predictors of the model, and t_α is the t value at confidence level α with $n-p$ degrees of freedom; in this study, $\alpha = 0.05$.

3. Results

3.1. Plot Size Effects on LiDAR-Derived Metrics

3.1.1. Height Metrics

Among the four datasets of the four quadrat combination protocols, the mean differences in LiDAR-derived height metrics (hp25, hp50, hp75, Hmean, Hmax, and Hcv) between plots of different sizes (600, 400, 300, 200, and 100 m²) and 900 m² plots were small for all forest types, and their standard deviations were approximately one order of magnitude larger than the mean differences. As the plot size increased, the mean of the differences showed irregular variations, while the standard deviations of the differences increased rapidly. Figure 3a shows the trends in mean and standard deviation (SD) of the difference in the Hmean between plots of different sizes and the 900 m² plot in the Chinese fir forests.

The paired t -tests were performed to assess the statistically significant differences in the means of differences in six LiDAR-derived height metrics for plots of different sizes (600 vs. 900 m², 400 vs. 900 m², 300 vs. 900 m², 200 vs. 900 m², and 100 vs. 900 m²) in each dataset. As there were four datasets, four tests were performed. Then, we counted the number of statistically significant differences ($\alpha = 0.05$) in these six metrics. The results were described as follows: (1) for all forest types, the number of statistically significant differences in Hmax between plots of different sizes and the 900 m² plot was all four, which implied that for all forest types, the mean of Hmax for all plots of different sizes differed significantly from that of the 900 m² plot; and (2) for the remaining five height metrics, the maximum number of significant differences was two, indicating that the means of these metrics were not statistically significantly different between plots of different sizes and the 900 m² plot for all forest types.

The LiDAR-derived height metrics varied with the area of the field plot and forest types. In all four datasets for the Chinese fir and eucalyptus forests, the means of Hmean did not differ significantly between plots of different sizes and the 900 m² plots, while the means of hp25, hp50, hp75, and Hcv had a few irregular statistically significant differences. For the pine forests, the means of hp75 were not significantly different among the field plots of different sizes, while the means of hp25, hp50, Hmean, and Hcv showed one to two statistically significant differences in four datasets, but these significant differences appeared in different datasets and without obvious regularity. There was no statistically significant difference in the mean of Hmean among the field plots of different sizes for the broad-leaved forests. The results for the remaining metrics were the same as the results for the pine forests. The variations in point cloud height metrics among field plots of the above-mentioned different sizes could be summarized as follows: (1) except for Hmax, the mean LiDAR-derived height metrics were not statistically significantly different between plots of different sizes and the 900 m² plot; (2) Hmean and Hcv were almost not statistically

significantly different between plot sizes; (3) the probabilities of statistically significant differences in laser point cloud height metrics for the pine and broad-leaved forests were higher than those for the Chinese fir and eucalyptus forests; and (4) the probabilities of statistically significant differences were considerably higher in the height metrics of the middle-to-low canopy layers (hp25 and hp50) than in the middle-to-upper canopy layers (hp75) (mainly for the pine forests).

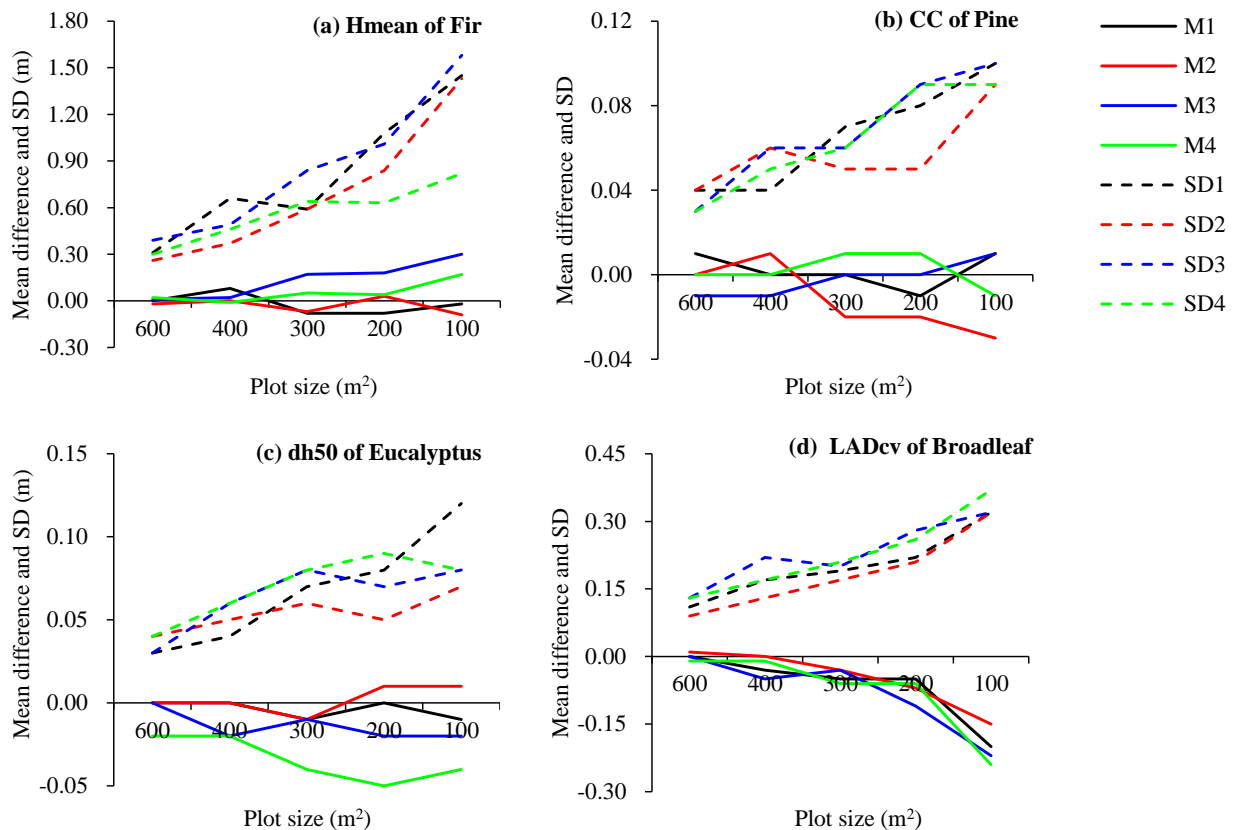


Figure 3. Mean and standard deviation of the difference in some LiDAR-derived metrics between plots of different sizes and the 900 m² plot. M1–M4 and SD1–SD4 were the mean differences and standard deviations for protocols 1–4, respectively. (a) Mean height of the Chinese fir forests, (b) canopy cover of the pine forests, (c) dp50 of the eucalyptus forests, and (d) LADcv of the broad-leaved forests.

The means of Hmax in all plot sizes differed statistically significantly from those in 900 m² plots, implying that Hmax was extremely unstable, and thus, unsuitable as a predictor for estimating forest attributes [9]. Additional analysis indicated that (Table 3): (1) as the plot size increased, the standard deviations of hp50 and Hmean for all forest types decreased gradually, and when the plot size was ≥ 400 m², the standard deviations of these two metrics were extremely close, decreasing slightly with increasing plot size; and (2) the standard deviations of Hcv remained constant for field plots of all sizes.

Table 3. Standard deviations of some LiDAR-derived metrics and measured forest attributes for field plots of different sizes.

Forest Type	Plot Size (m ²)	hp50	Hmean	Hcv	CC	dp50	LADcv	H	VOL	BA
Fir	100	2.50	1.93	0.16	0.15	0.17	0.37	2.62	68.49	7.35
	200	1.92	1.62	0.15	0.13	0.17	0.29	2.18	54.82	5.91
	300	1.81	1.50	0.15	0.14	0.16	0.26	2.05	50.46	5.48
	400	1.34	1.39	0.14	0.13	0.15	0.23	1.88	45.66	5.12
	600	1.31	1.36	0.14	0.13	0.15	0.23	1.81	44.73	5.01
	900	1.29	1.34	0.14	0.14	0.16	0.23	1.81	43.86	4.89
Pine	100	5.08	3.88	0.19	0.17	0.22	0.45	3.67	90.63	10.43
	200	4.46	3.80	0.17	0.15	0.21	0.36	3.55	79.54	8.48
	300	4.34	3.80	0.16	0.14	0.20	0.33	3.55	78.11	8.26
	400	4.40	3.82	0.15	0.13	0.21	0.31	3.65	75.79	7.98
	600	4.38	3.80	0.15	0.13	0.20	0.30	3.54	74.80	7.75
	900	4.36	3.78	0.14	0.12	0.20	0.29	3.56	74.45	7.61
Eucalyptus	100	5.95	3.73	0.13	0.22	0.16	0.62	3.57	76.16	7.05
	200	5.42	3.63	0.13	0.22	0.15	0.55	3.42	74.06	6.62
	300	5.51	3.59	0.13	0.22	0.15	0.50	3.41	73.73	6.52
	400	5.24	3.59	0.13	0.21	0.15	0.46	3.56	71.80	6.22
	600	5.04	3.49	0.12	0.21	0.14	0.47	3.43	72.15	6.25
	900	4.77	3.37	0.12	0.21	0.14	0.46	3.41	72.09	6.23
Broad-leaved	100	5.85	5.47	0.21	0.19	0.26	0.34	4.04	93.61	9.90
	200	5.47	5.34	0.20	0.19	0.26	0.27	3.92	83.39	8.90
	300	5.50	5.36	0.20	0.19	0.27	0.25	3.85	81.65	8.44
	400	5.52	5.37	0.21	0.19	0.27	0.24	3.79	79.89	8.34
	600	5.51	5.35	0.20	0.19	0.27	0.22	3.72	77.72	8.12
	900	5.51	5.34	0.20	0.18	0.28	0.22	3.66	76.25	8.03

3.1.2. Density Metrics

Similar to the height metrics, the differences in mean of all density metrics (CC, dp25, dp50, and dp75) between plots of different sizes and the 900 m² plots were small for all forest types. Their standard deviations of the differences were approximately one order of magnitude larger than their mean differences. The mean differences changed irregularly as the plot size decreased from 600 m² to 100 m², while their standard deviations tended to increase rapidly. Figure 3b shows the variations in mean and standard deviation of the differences in CC between plots of different sizes and the 900 m² plots in the pine forests, and Figure 3c shows the same variations in dp50 in the eucalyptus forests.

For all forest types, the means and standard deviations of the difference in CC between plots of different sizes and the 900 m² plots were the smallest among all density metrics. In the pine and eucalyptus forests, two and one statistically significant differences were found, respectively. The mean dp25 had one to two statistically significant differences in the 300, 200, and 100 m² plots in the pine forests. These results showed that, for all four forest types, there were not any statistically significant differences in CC and dp25 between plots of different sizes and the 900 m² plots. For dp50 in the fir, pine, and broad-leaved forests, one to four statistically significant differences were observed between plots of different sizes and the 900 m² plots, indicating that dp50 varied widely among the plots of different sizes for these forest types. For the Chinese fir, pine, and broad-leaved forests, when plot size was less than or equal to 400 m², four statistically significant differences were found for dp75, which revealed that in all four datasets of these three forest types, dp75 differed significantly between plots smaller than or equal to 400 m² and the 900 m² plot. There were two or three statistically significant differences in dp75 of the 600 m² plots. In the eucalyptus forest, no statistically significant difference in dp75 occurred in the 600 m² plots, but 1–2 statistically significant differences were noted in plots of other sizes. The above results of paired *t*-tests for density metrics of plots of different sizes can

be summarized as follows: (1) for CC and density percentile of the lower layer (dp25), no forest type had regular statistically significant differences between plots of different sizes and 900 m² plots, but the density percentile of the upper layer (dp75) was not the same (except for the eucalyptus forest); (2) for dp50, all forest types other than the eucalyptus forest had some statistically significant differences between plots of different sizes and the 900 m² plots, although they were irregular.

For all four forest types, the standard deviations of the main density metrics (CC and dp50) remained approximately constant among the plots of different sizes (Table 3).

3.1.3. Vertical Structure Metrics

Unlike the height and density metrics, the mean differences in vertical structure metrics (e.g., the LADmean and LADcv) of all forest types between plots of different sizes and the 900 m² plots decreased gradually as the plot size decreased, and their standard deviations increased rapidly. Figure 3d shows how the means and standard deviations of the differences in LADcv in the broad-leaved forests varied with a decrease in plot size. When the plot size increased from 100 m² to 900 m², the standard deviations of LADcv of all forest types gradually decreased, as the plot area was greater than or equal to 400 m², they were close to each other (Table 3).

In four datasets, two to four statistically significant differences were found in the means LADmean between the plots of different sizes and the 900 m² plots in the pine and broad-leaved forests, indicating that, in these two types of forests, the mean LADmean of the plots of different sizes differed significantly from those of the 900 m² plots. In the Chinese fir forests, there was no statistically significant difference between plots of 600 m² and 900 m² for LADmean, while there were one to three statistically significant differences for plots of other sizes. Eucalyptus forests did not significantly differ from 900 m² plots in terms of LADmean, as plot sizes were greater than or equal to 300 m². There was no statistically significant difference in LADcv between plots of the following sizes and the 900 m² plots: less than or equal to 200 m² for the eucalyptus and broad-leaved forests and greater than or equal to 400 m² for the pine forests. In plots of other sizes for these three forest types, and plots of all sizes for the fir forests, there were one to four statistically significant differences in LADcv. These results suggested that the vertical structure of the stand canopies was more homogeneous in the eucalyptus and broad-leaved forests than in the pine and Chinese fir forests.

3.2. Plot Size Effects on Measured Forest Attributes

The mean differences in measured forest attributes (DBH, H, Hm, BA, and VOL) between plots of different sizes and the 900 m² plots of all four forest types were minor and varied irregularly as the plot size decreased. However, their standard deviations of the differences were considered great and increased rapidly with a decreasing plot size (Figure 4).

For four forest types, the results of paired *t*-tests showed that the means of Hm of plots of different sizes were statistically significantly different ($\alpha = 0.05$) from that of 900 m² plots in most of the datasets. Among other forest attributes, significant differences were noted in only a few datasets. These results suggested that, except for the means of Hm, there was little or no significant difference in measured forest attributes between plots of different sizes and 900 m² plots.

For all forest types, as the plot size increased from 100 m² to 900 m², the standard deviations of the main stand attributes (H, VOL, and BA) were found to decrease gradually (Table 3), suggesting that with increasing plot size, the variation in the forest attributes decreased.

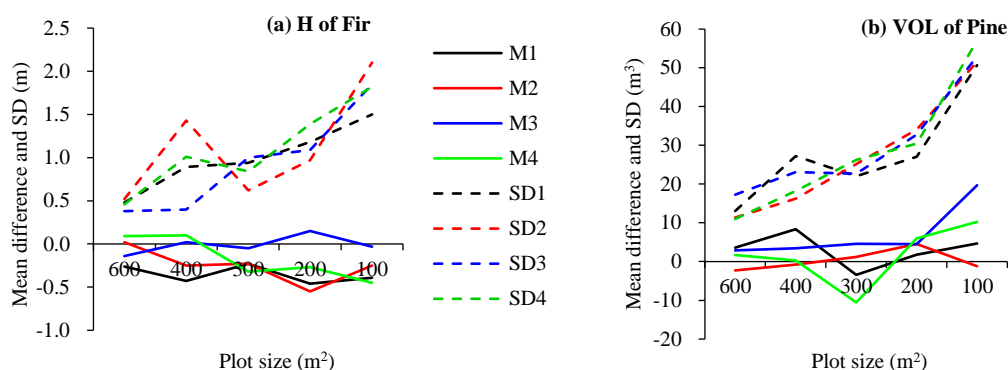


Figure 4. Means and standard deviations of the differences in measured forest attributes between plots of different sizes and 900 m² plots. M1–M4 and SD1–SD4 are the mean differences and their standard differences for protocols 1–4, respectively. (a) mean height of the Chinese fir forests, and (b) stand volume of the pine forests.

3.3. Plot Size Effects on the Performances of the Predictive Models of Forest Attributes

Typically, the differences in estimated VOL and BA between plots of different sizes and 900 m² plots decreased with an increasing plot size for all four forest types, and the differences in estimated VOL were greater than those in estimated BA. The greatest differences in estimated VOL and BA in the fir forests were 7.38% and −7.6%, respectively; in the pine forests, they were −14.38% and −8.66%; in the eucalyptus forests, they were −12.57% and −9.48%; in the broad-leaved forests, they were −10.07% and −8.20%. Additionally, the standard deviations of the estimated VOL and BA increased for all forest types as the plot size decreased.

For all four forest types, the results of paired *t*-tests indicated that although some statistically significant differences ($\alpha = 0.05$) in the means of the estimated VOL and BA appeared between several plots of different sizes and 900 m² plots in some datasets, these differences were irregular. Overall, the means of estimated VOL and BA for plots of different sizes did not differ statistically significantly from those of the 900 m² plots. However, after calculating the means of goodness-of-fit statistics and VOL and BA estimation accuracy, we found that as the plot size increased, the R² of all VOL and BA predictive models increased gradually, while rRMSE and MPE decreased incrementally (Table 4). As the plot size increased from 100 m² to 900 m², the accuracy of VOL and BA estimation gradually improved.

As the plot size increased from 100 m² to 200 m², the R² values of VOL and BA estimations had the greatest increase for all forest types, while the rRMSE and MPE had the greatest decrease. For all forest types, the rRMSE and MPE values of VOL and BA estimations showed essentially the same trend for plot sizes greater than or equal to 200 m². These results indicated that the effect of plot size on estimation accuracy was similar for different attributes and forest types.

Zolkos et al. summarized more than 30 research papers on discrete LiDAR forest biomass estimation and concluded that the residual standard errors (RSE (%)) and plot sizes had a logarithmic relationship [18]. However, we found that the multiplicative power model ($\text{rRMSE}(\%) = a_0 A^{a_1}$, where *A* is the plot size in ha, *a*₀ and *a*₁ are the model parameters) was most suitable for fitting the relationships between the values of rRMSE of the VOL and BA estimations and plot sizes for four forest types (Table 5).

The values of *a*₁ in the rRMSE-*A* model for stand volume estimation were fairly close to each other for all four forest types, except for the pine forests, indicating that their rRMSE trends were quite similar as the plot size increased. In the rRMSE-*A* model for the basal area estimation, the values of *a*₁ for the fir and eucalyptus forests and the values of *a*₁ for the pine and broadleaf forests were comparatively close, indicating a similar trend in their rRMSEs with an increasing plot size. Overall, decreasing trends in rRMSE of VOL and BA estimation were essentially the same in all forest types as the plot size increased (Figure 5).

Table 4. Means of R^2 , rRMSE, and MPE for the predictive models of VOL and BA in plots of various sizes in the four datasets of four forest types.

Stratum	Plot Size (m ²)	VOL			BA		
		R ²	rRMSE (%)	MPE (%)	R ²	rRMSE (%)	MPE (%)
Fir	100	0.390	29.31	13.93	0.313	25.00	11.88
	200	0.433	22.38	10.64	0.310	19.77	9.40
	300	0.354	21.56	10.25	0.211	19.21	9.13
	400	0.424	19.07	9.07	0.327	17.10	8.13
	600	0.467	18.11	8.61	0.337	16.55	7.87
	900	0.554	16.28	7.74	0.378	15.58	7.41
Pine	100	0.327	43.69	17.48	0.098	37.88	15.15
	200	0.445	34.13	13.66	0.172	29.34	11.74
	300	0.527	30.73	12.29	0.247	27.13	10.86
	400	0.517	30.41	12.17	0.235	26.53	10.61
	600	0.572	28.06	11.23	0.302	24.51	9.81
	900	0.596	26.93	10.77	0.331	23.46	9.39
Eucalyptus	100	0.669	30.75	13.48	0.569	26.96	11.81
	200	0.772	24.48	10.73	0.710	20.42	8.95
	300	0.812	22.05	9.66	0.770	17.90	7.85
	400	0.864	18.26	8.00	0.823	15.03	6.59
	600	0.877	17.37	7.61	0.835	14.45	6.33
	900	0.905	15.18	6.65	0.876	12.46	5.46
Broad-leaved	100	0.698	38.73	15.83	0.560	31.45	12.85
	200	0.779	30.84	12.60	0.657	25.68	10.49
	300	0.788	28.89	11.81	0.668	23.46	9.59
	400	0.802	27.43	11.21	0.665	23.73	9.70
	600	0.821	25.37	10.37	0.668	22.94	9.37
	900	0.847	23.13	9.45	0.690	21.89	8.94

Table 5. Parameter estimates of the multiplicative power regression models for the relationship between rRMSE (%) and plot size (ha) and their goodness-of-fit statistics.

Attribute	Forest Type	a_0	a_1	R ²	rRMSE (%)
VOL	Fir	6.4570	−0.3574	0.890	11.40
	Pine	13.7107	−0.2637	0.772	11.02
	Eucalyptus	7.0049	−0.3422	0.828	13.79
	Broad-leaved	10.2562	−0.3360	0.879	13.19
BA	Fir	6.7816	−0.3109	0.811	11.87
	Pine	11.3946	−0.2706	0.608	9.64
	Eucalyptus	5.8844	−0.3186	0.842	11.34
	Broad-leaved	11.4020	−0.2745	0.735	15.85

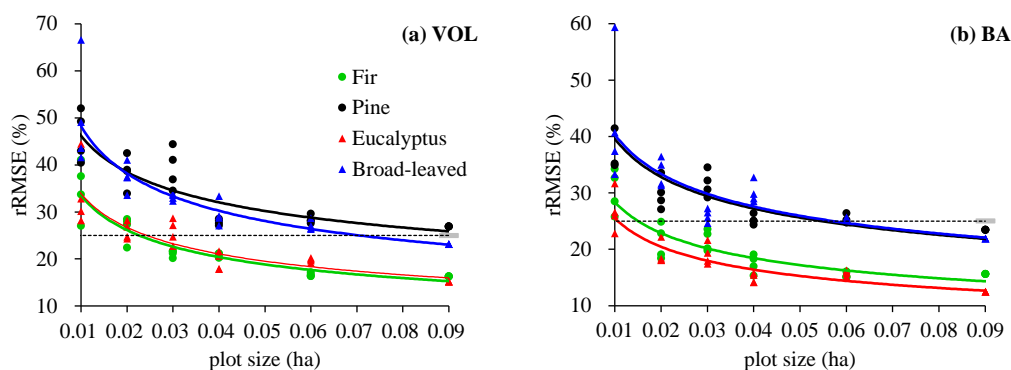


Figure 5. Regression relationships between the rRMSE of the VOL (a) and BA (b) estimation models and plot sizes (ha) for four forest types.

The theoretical differences in rRMSE of VOL and BA estimation between plots of different sizes and the 900 m² plots were derived based on the regression relationships between rRMSEs of VOL and BA estimation models and plot sizes described above. The differences in rRMSEs of VOL estimation between 600 m² and 900 m² plots for all four forest types were approximately 15%, whereas the differences in BA estimation were all less than 14% (Table 6). Between the plots of various sizes and the 900 m² plots, there were some differences between the theoretical (Table 6) and average differences (Table 5) in the rRMSEs of VOL and BA estimation.

Table 6. Theoretical difference (%) of rRMSEs between plots of different sizes and the 900 m² plots calculated from the rRMSE plot size regression models in VOL and BA estimation in four forest types.

Plot Size (m ²)	rRMSE Difference (%) in VOL Estimation				rRMSE Difference (%) in BA Estimation			
	Fir	Pine	Eucalyptus	Broad-Leaved	Fir	Pine	Eucalyptus	Broad-Leaved
100	119.3	78.5	112.1	109.2	98.0	83.4	101.4	82.8
200	71.2	48.7	67.3	65.8	59.6	51.5	61.5	51.1
300	48.1	33.6	45.6	44.6	40.7	35.4	41.9	35.2
400	33.6	23.8	32.0	31.3	28.7	25.1	29.5	24.9
500	23.4	16.8	22.3	21.8	20.1	17.6	20.6	17.5
600	15.6	11.3	14.9	14.6	13.4	11.8	13.8	11.8
700	9.4	6.9	9.0	8.8	8.1	7.2	8.3	7.1
800	4.3	3.2	4.1	4.0	3.7	3.3	3.8	3.3

4. Discussion

Some studies have demonstrated that increasing plot size helps to improve the accuracy of airborne LIDAR-based forest attribute estimation [1,11,12,18,31–36]. Our study also supports these findings and provides new evidence for subtropical planted forests. Most importantly, we have preliminarily revealed the mechanism of the effect of plot size on forest attribute estimation.

Existing studies have generally agreed that plot sizes affect the accuracy of forest attribute estimation using LiDAR data because of the following main factors: (1) a large plot captures an adequate amount of on-ground (in situ) structure variability [37], thereby providing a more accurate representation of the mean values of forest attributes [36]; (2) positioning errors in plots constantly exist, and a large plot maintains a greater amount of spatial overlap between ground-reference and LiDAR data for any given co-registration error [38], which can effectively reduce the ill effects of co-registration error [31]; and (3) a large plot has a lower perimeter-to-area ratio, which helps to reduce the relative size of the random error component associated with edge-induced noise [31].

In this study, although the LiDAR metrics and measured forest attributes were close among plots of different sizes, as the plot size decreased, the standard deviation increased rapidly (Figures 3 and 4, Table 3). The main reasons for these findings are that a small plot encloses fewer trees, resulting in high homogeneity within the plot. Nevertheless, in a highly heterogeneous population, there is great variation among plots. In contrast, a large plot encloses more trees and has high heterogeneity among plots; because of spatial averaging [18,39], the variability among plots is reduced. Variations in LiDAR variables and measured forest attributes among plots tend to decrease gradually as the plot area increases, which leads to a decrease in the standard deviation of the response variables and independent variables of the estimated models of forest attributes. Assuming that a close regression relationship between the target forest attributes and LiDAR variables exists in the population, model accuracy improves as variances in the dependent and independent variables decrease. Therefore, we believe that spatial averaging is the main reason for the improved model accuracy with an increasing plot size.

Determining the plot size in an operational forest inventory is a difficult process, and we have to reach a more favorable trade-off between the estimation accuracy of forest attributes and measurement cost per plot. In short, a suitable plot size at an acceptable

cost has to be found. Most plot sizes in published research were less than 600 m² [12]. Our study indicated that for the given point density (3.2 points m⁻²) and the number of field plots (Table 1), the trends in improvement of VOL and BA estimation accuracy as the plot size increased were essentially the same for all forest types (Table 4 and Figure 5). The estimation accuracy of forest attributes is closely related to the extent of the study area and the complexity of the forest context, the number of plots, plot sizes, modeling methods, and sampling strategies or approaches. In 34 studies worldwide, the mean residual standard error (RSE) of discrete airborne LiDAR-based aboveground biomass estimation was 27% [18]. In our other study on a large scale (2.21 × 10⁶ ha), which was essentially centered on the present study site, the rRMSEs for VOL estimation of four forest types (the plot sizes were 600 m², the numbers of sample plots for four forest types were 84, 97, 107, and 95, respectively; the pine and broad-leaved forests were mostly natural mixed forests) were 20.89%, 21.69%, 18.53%, and 36.32%, respectively [28], and the model accuracy was lower than those of the present study, except for the pine forests. The main reasons are the limited extent of the present study site and the high homogeneity of the forest structure. Therefore, based on the results of the present study, it is difficult to determine the most appropriate set of plot sizes for estimating forest attributes for different forest types in a larger study area. Assuming that an accuracy of 15% lower than the highest accuracy is acceptable in forest attribute estimation; we believe that a 600 m² plot is appropriate for all forest types, and at this point, the cost of the plot measurement is approximately one-third lower than that of the 900 m² plots.

Most field plots in previous studies on this topic were circular [1,12]. In this study, we focused on rectangular plots. Circular plots have the advantage that plots of different sizes completely overlap in the central region, and plot data are highly comparable. Its disadvantage is that it is difficult to identify plot boundaries in fieldwork. Tropical and subtropical montane or hilly terrain, in particular, are characterized by extreme variations in slope surfaces and lush understory vegetation, making it extremely difficult to set and measure a circular plot. The advantage of rectangular plots is that they make plot establishment in fieldwork simple and accurate, thus, ensuring data accuracy. The disadvantage is that the overlap is not in the center of the plot because of an inadequate overlap among plots of different sizes (Figure 1), resulting in slightly less comparable data among plots. Nevertheless, the rectangular plot has traditionally been used in the continuous national forest inventory (NFI) and operational forest management inventory (FMI) in China. However, the number of field plots in this study is small for all forest types, there are only six different plot sizes due to the limitations of the quadrat combinations in rectangular plots, and the study is focused only on the planted forests. Therefore, future work should expand the study area to cover more forest types (e.g., natural forests), increase the number of plots, and increase the number of plots of different sizes.

5. Conclusions

From the analysis presented in this paper, we had drawn the following conclusions:

- (1) The means of the 25th, 50th, and 75th height percentiles of laser point clouds, Hmean, Hcv, CC, 25th and 50th density percentiles, and LADcv of plots of different sizes for all four forest types showed irregular differences or no statistically significant difference from that of the 900 m² plots. However, their standard deviations decreased as the plot size increased. In general, statistically significant differences in the means of Hmax, LADmean, and 75th density percentile were found between plots of various sizes and 900 m² plots.
- (2) Except for the mean Hm, the measured forest attributes of plots of different sizes for all four forest types exhibited irregular variations and no statistically significant difference from those of the 900 m² plots. However, their standard deviations decreased with the increasing plot size.
- (3) As the plot size increased from 100 m² to 900 m², the predictive errors (MPE and rRMSE) decreased at approximately the same rate for all forest types, and the model

accuracies gradually improved at a similar rate for all forest types. These results were most likely due to the fact that the standard deviations of the LiDAR-derived metrics and measured forest attributes decreased as the plot size increased; that is, the variation in the independent and dependent variables of the model decreased with the increasing plot size, which improved the robustness of the model.

- (4) According to this paper, we preliminarily recommend that for a large-scale subtropical planted forest inventory, the plot sizes should be at least 600 m² for all forest types.

Author Contributions: C.L.: conceptualization, methodology, calculation, data collection and analysis, writing—original draft—review and editing, project administration, funding acquisition. X.L.: calculation, writing—original draft. H.D.: conceptualization, funding acquisition. Z.L.: calculation. M.Z.: calculation. All authors have read and agreed to the published version of the manuscript.

Funding: This study received financial support from Guangxi Forest Inventory and Planning Institute (GXLKYKJ201601).

Data Availability Statement: The original data are available from the corresponding author.

Acknowledgments: This is a pre-research project of the Fifth Forest Management Inventory Project of Guangxi Zhuang Autonomous Region, China (2017–2020). The authors would like to express their sincere gratitude to Chengling Yang and Yao Liang and 25 other colleagues from the Guangxi Forest Inventory and Planning Institute (FIPI-GX) who worked on the field plot measurements. The authors also thank Guangxi 3D Remote Sensing Engineering Technology Co., Ltd., which was responsible for airborne LiDAR data acquisition and preprocessing.

Conflicts of Interest: The authors declare no conflict of interest.

References

- Watt, M.; Adams, T.; Aracil, S.G.; Marshall, H.; Watt, P. The influence of LiDAR pulse density and plot size on the accuracy of New Zealand plantation stand volume equations. *N. Z. J. For. Sci.* **2013**, *43*, 15. [\[CrossRef\]](#)
- Bouvier, M.; Durrieu, S.; Fournier, R.A.; Renaud, J.-P. Generalizing predictive models of forest inventory attributes using an area-based approach with airborne LiDAR data. *Remote Sens. Environ.* **2015**, *156*, 322–334. [\[CrossRef\]](#)
- Hyyppä, J.; Yu, X.; Hyyppä, H.; Vastaranta, M.; Holopainen, M.; Kukko, A.; Kaartinen, H.; Jaakkola, A.; Vaaja, M.; Koskinen, J.; et al. Advances in forest inventory using airborne laser scanning. *Remote Sens.* **2012**, *4*, 1190–1207. [\[CrossRef\]](#)
- Næsset, E. Airborne laser scanning as a method in operational forest inventory: Status of accuracy assessments accomplished in Scandinavia. *Scand. J. For. Res.* **2007**, *22*, 433–442. [\[CrossRef\]](#)
- Packalen, P.; Maltamo, M. Species-specific management inventory in Finland. In *Forestry Applications of Airborne Laser Scanning: Concepts and Case Studies, Managing Forest Ecosystems 27*; Maltamo, M., Næsset, E., Vauhkonen, J., Eds.; Springer: Dordrecht, The Netherlands, 2014; pp. 241–252. [\[CrossRef\]](#)
- White, J.C.; Tompalski, P.; Vastaranta, M.; Wulder, M.A.; Saarinen, N.; Stepper, C.; Coops, N.C. *A Model Development and Application Guide for Generating an Enhanced Forest Inventory Using Airborne Laser Scanning Data and an Area-Based Approach*; Canadian Wood Fibre Centre: Victoria, BC, Canada, 2017. [\[CrossRef\]](#)
- Lin, C.; Thomson, G.; Popescu, S.C. An IPCC-compliant technique for forest carbon stock assessment using airborne LiDAR-derived tree metrics and competition index. *Remote Sens.* **2016**, *8*, 528. [\[CrossRef\]](#)
- Lo, C.S.; Lin, C. Growth-competition-based stem diameter and volume modeling for tree-level forest inventory using airborne LiDAR data. *IEEE T Geosci. Remote* **2012**, *51*, 2216–2226. [\[CrossRef\]](#)
- Pourreza, M.; Moradi, F.; Khosravi, M.; Deljouei, A.; Vanderhoof, M.K. GCPs-free photogrammetry for estimating tree height and crown diameter in Arizona Cypress plantation using UAV-mounted GNSS RTK. *Forests* **2022**, *13*, 1905. [\[CrossRef\]](#)
- Štroner, M.; Urban, R.; Seidl, J.; Reindl, T.; Brouček, J. Photogrammetry using UAV-mounted GNSS RTK: Georeferencing strategies without GCPs. *Remote Sens.* **2021**, *13*, 1336. [\[CrossRef\]](#)
- Gobakken, T.; Næsset, E. Assessing effects of laser point density, ground sampling intensity, and field sample plot size on biophysical stand properties derived from airborne laser scanner data. *Can. J. For. Res.* **2008**, *38*, 1095–1109. [\[CrossRef\]](#)
- Ruiz, L.A.; Hermosilla, T.; Mauro, F.; Godino, M. Analysis of the influence of plot size and LiDAR density on forest structure attribute estimates. *Forests* **2014**, *5*, 936–951. [\[CrossRef\]](#)
- Singh, K.; Chen, G.; Vogler, J.B.; Meentemeyer, R.K. When big data are too much: Effects of LiDAR returns and point density on estimation of forest biomass. *J. Sel. Top. Appl. Earth Obs. Remote Sens.* **2016**, *9*, 3210–3218. [\[CrossRef\]](#)
- Næsset, E. Area-based inventory in Norway—From innovation to an operation reality. In *Forestry Applications of Airborne Laser Scanning: Concepts and Case Studies, Managing Forest Ecosystems 27*; Maltamo, M., Næsset, E., Vauhkonen, J., Eds.; Springer: Dordrecht, The Netherlands, 2014; pp. 215–240. [\[CrossRef\]](#)

15. Stereńczak, K.; Lisańczuk, M.; Parkitna, K.; Mitelsztedt, K.; Mroczek, P.; Miscicki, S. The influence of number and size of sample plots on modeling growing stock volume based on airborne laser scanning. *Drewno* **2018**, *61*. [[CrossRef](#)]
16. Næsset, E. Predicting forest stand characteristics with airborne scanning laser using a practical two-stage procedure and field data. *Remote Sens. Environ.* **2002**, *80*, 88–99. [[CrossRef](#)]
17. Næsset, E.; Gobakken, T. Estimation of above- and below-ground biomass across regions of the boreal forest zone using airborne laser. *Remote Sens. Environ.* **2008**, *112*, 3079–3090. [[CrossRef](#)]
18. Zolkos, S.G.; Goetz, S.J.; Dubayah, R. A meta-analysis of terrestrial aboveground biomass estimation using lidar remote sensing. *Remote Sens. Environ.* **2013**, *128*, 289–298. [[CrossRef](#)]
19. Liao, Z.; Huang, D. *Forest inventory handbook of Guangxi, China*; Forestry Department of Guangxi Zhuang Autonomous Region: Nanning, China, 1986. (In Chinese)
20. Nie, S.; Wang, C.; Zeng, H.; Xi, X.; Li, G. Above-ground biomass estimation using airborne discrete-return and full-waveform LiDAR data in a coniferous forest. *Ecol. Indic.* **2017**, *78*, 221–228. [[CrossRef](#)]
21. Chen, Q.; Laurin, G.V.; Battles, J.J.; Saah, D. Integration of airborne LiDAR and vegetation types derived from aerial photography for mapping aboveground live biomass. *Remote Sens. Environ.* **2012**, *121*, 108–117. [[CrossRef](#)]
22. Kim, E.; Lee, W.-K.; Yoon, M.; Lee, J.-Y.; Son, Y.; Abu Salim, K. Estimation of voxel based above-ground biomass using airborne LiDAR data in an intact tropical Rain Forest, Brunei. *Forests* **2016**, *7*, 259. [[CrossRef](#)]
23. Silva, V.S.D.; Silva, C.A.; Mohan, M.; Cardil, A.; Rex, F.E.; Loureiro, G.H.; Almeida, D.R.A.D.; Broadbent, E.N.; Gorgens, E.B.; Dalla Corte, A.P.; et al. Combined impact of sample size and modeling approaches for predicting stem volume in *Eucalyptus* spp. forest plantations using field and LiDAR Data. *Remote Sens.* **2020**, *12*, 1438. [[CrossRef](#)]
24. Asner, G.P.; Mascaró, J.; Muller-Landau, H.C.; Vieilledent, G.; Vaudry, R.; Rasamoelina, M.; Hall, J.S.; van Breugel, M. A universal airborne LiDAR approach for tropical forest carbon mapping. *Oecologia* **2012**, *168*, 1147–1160. [[CrossRef](#)]
25. Treitz, P.; Lim, K.; Woods, M.; Pitt, D.; Nesbitt, D.; Etheridge, D. LiDAR sampling density for forest resource inventories in Ontario, Canada. *Remote Sens.* **2012**, *4*, 830–848. [[CrossRef](#)]
26. Nilsson, M.; Nordkvist, K.; Jonzén, J.; Lindgren, N.; Axensten, P.; Wallerman, J.; Egberth, M.; Larsson, S.; Nilsson, L.; Eriksson, J.; et al. A nationwide forest attribute map of Sweden predicted using airborne laser scanning data and field data from the National Forest Inventory. *Remote Sens. Environ.* **2017**, *194*, 447–454. [[CrossRef](#)]
27. Knapp, N.; Fischer, R.; Cazcarra-Bes, V.; Huth, A. Structure metrics to generalize biomass estimation from lidar across forest types from different continents. *Remote Sens. Environ.* **2020**, *237*, 111597. [[CrossRef](#)]
28. Li, C.; Li, Z. Generalizing predictive models of sub-tropical forest inventory attributes using an area-based approach with airborne LiDAR data. *Sci. Silvae Sin.* **2021**, *57*, 23–35. (In Chinese) [[CrossRef](#)]
29. Zeng, W.; Duo, H.; Lei, X.; Chen, X. Individual tree biomass equations and growth models sensitive to climate variables for *Larix* spp. in China. *Eur. J. For. Res.* **2017**, *136*, 233–249. [[CrossRef](#)]
30. Zeng, W.; Fu, L.; Xu, M.; Wang, X.; Chen, Z.; Yao, S. Developing individual tree-based models for estimating aboveground biomass of five key coniferous species in China. *J. For. Res.* **2018**, *29*, 1251–1261. [[CrossRef](#)]
31. Frazer, G.W.; Magnussen, S.; Wulder, M.A.; Niemann, K.O. Simulated impact of sample plot size and co-registration error on the accuracy and uncertainty of LiDAR-derived estimates of forest stand biomass. *Remote Sens. Environ.* **2021**, *115*, 636–649. [[CrossRef](#)]
32. Næsset, E.; Bollandsas, O.M.; Gobakken, T.; Solberg, S.; McRoberts, R.E. The effects of field plot size on model-assisted estimation of aboveground biomass change using multitemporal interferometric SAR and airborne laser scanning data. *Remote Sens. Environ.* **2015**, *168*, 252–264. [[CrossRef](#)]
33. Asner, G.P.; Mascaró, J. Mapping tropical forest carbon: Calibrating plot estimates to a simple LiDAR metric. *Remote Sens. Environ.* **2014**, *140*, 614–624. [[CrossRef](#)]
34. Mauya, E.; Hansen, E.; Gobakken, T.; Bollandsås, O.; Malimbwi, R.; Næsset, E. Effects of field plot size on prediction accuracy of aboveground biomass in airborne laser scanning-assisted inventories in tropical rainforests of Tanzania. *Carbon Balance Manag.* **2015**, *10*, 10. [[CrossRef](#)]
35. Kachamba, D.J.; Ørka, H.O.; Næsset, E.; Eid, T.; Gobakken, T. Influence of plot size on efficiency of biomass estimates in inventories of dry tropical forests assisted by photogrammetric data from an unmanned aircraft system. *Remote Sens.* **2017**, *9*, 610. [[CrossRef](#)]
36. Hernández-Stefanoni, J.L.; Reyes-Palomeque, G.; Castillo-Santiago, M.Á.; George-Chacón, S.P.; Huechacona-Ruiz, A.H.; Tun-Dzul, F.; Rondon-Rivera, D.; Dupuy, J.M. Effects of sample plot size and GPS location errors on aboveground biomass estimates from LiDAR in tropical dry forests. *Remote Sens.* **2018**, *10*, 1586. [[CrossRef](#)]
37. Zenner, E.K. Investigating scale-dependent stand heterogeneity with structure-area-curves. *For. Ecol. Manag.* **2005**, *209*, 87–100. [[CrossRef](#)]
38. Flewelling, J.W. Plot size, shape, and co-registration error determine expected overlap. In Proceedings of the International Union of Forest Research Organizations (IUFRO), Division 4, Extending Forest Inventory and Monitoring Over Space and Time, Quebec City, QC, Canada, 19–22 May 2009. Available online: <https://blue.for.msu.edu/meeting/proc2/Flewelling.pdf> (accessed on 28 April 2010).
39. Mitchard, E.T.A.; Saatchi, S.S.; Baccini, A.; Asner, G.P.; Goetz, S.J.; Harris, N.L.; Sandra, B. Uncertainty in the spatial distribution of tropical forest biomass: A comparison of pan-tropical maps. *Carbon Balance Manag.* **2013**, *8*, 10. [[CrossRef](#)] [[PubMed](#)]